New insight to superoxide radical–mediated degradation of pentachlorophenate: Kinetic determination and theoretical calculations

Electronic Supplementary Material

Lu Bai[a,b], Lei He[a,b], Yifu Fu[a,b], Chu Chu[a,b], Zongsu Wei[c], Richard Spinney[d], Dionysios D. Dionysiou[e], Yanjie Liang[a,b], and Ruiyang Xiao*[a,b]

[a]Institute of Environmental Engineering, School of Metallurgy and Environment, Central South University, Changsha, 410083, China

[b]Chinese National Engineering Research Center for Control & Treatment of Heavy Metal Pollution, Changsha, 410083, China

[c]Centre for Water Technology (WATEC) & Department of Biological and Chemical Engineering, Aarhus University, Universitetsbyen, 8000 Aarhus C, Denmark

[d]Department of Chemistry and Biochemistry, The Ohio State University, Columbus, Ohio, 43210, U.S.A.

[e]Environmental Engineering and Science Program, University of Cincinnati, Cincinnati, Ohio, 45221, U.S.A.

Materials and methods

Chemicals. Hydrogen peroxide solution (H_2O_2, 30 *wt.* % in H_2O) was purchased from Aladdin (China). Sodium formate (FA, >99.0%), sodium dihydrogen phosphate (>99.0%), dibasic sodium phosphate (>99.0%), diethylenetriaminepentaacetic acid (DTPA), and adrenaline (Adr) were purchased from Sigma−Aldrich (China). Sodium pentachlorophenate (NaPCP) was purchased from Changping Shiying Chemicals.

Since the pK_a of PCP was reported to be 4.9,[1] PCP^- is the dominant species under the experimental condition (*i.e.*, pH = 8) (Fig. S2). All chemical reagents were used without further purification. All solutions were prepared using ultrapure water (ZWM-PA1-40, ZOOMAC, China) with the resistivity of 18.2 MΩ cm at 25 °C. A pH meter (PHSJ−4F, Leici, China) was used to measure solution pH.

Experimental procedures. The *in situ* long–path spectroscopic system and the non-steady state approach used to generate $O_2^{\bullet-}$ in aqueous solutions were described in our previous study in great detail.[2] Briefly, the *in situ* long–path spectroscopic system consists of a UV–Vis spectrometer (QE65PRO–ABS, Ocean Optics, USA) and a homemade quartz cell (6 cm × 4 cm × 5 cm). The generation of $O_2^{\bullet-}$ was achieved by irradiation for 60 s in a mixed solution by a 10 W low pressure ultraviolet (UV) lamp (GPH212T5L/4, Heraeus, Germany) with emission of monochromatic wavelength at 254 nm. The working solutions containing H_2O_2, FA, and DTPA were adjusted to pH 8 using phosphate buffer. Our preliminary result demonstrated that phosphate buffer exhibits no effects on formation and determination. H_2O_2 and FA serve as precursors of $O_2^{\bullet-}$ (see eqn.1 to 3).

$$H_2O_2 \xrightarrow{h\nu} {}^{\bullet}OH \quad (1)$$

$${}^{\bullet}OH + HCOO^- \rightarrow H_2O + CO_2^{\bullet-} \quad (2)$$

$$CO_2^{\bullet-} + O_2 \rightarrow CO_2 + O_2^{\bullet-} \quad (3)$$

Under the irradiation of UV light, H_2O_2 was photolyzed forming ${}^{\bullet}OH$ (eqn. 1). Subsequently, ${}^{\bullet}OH$ reacts with FA, converting it to reductive intermediate species, (*i.e.*, $CO_2^{\bullet-}$, eqn. 2). With dissolved dioxygen in solution, $CO_2^{\bullet-}$ transfers an electron to O_2 forming $O_2^{\bullet-}$ (eqn. 3).

DTPA was added to sequester the effects of catalyzing the disproportionation of $O_2^{\bullet-}$ due to the presence of trace metals (*e.g.*, Fe^{3+}, Cu^{2+}, *etc.*).[3] In every run, freshly prepared $O_2^{\bullet-}$ working solutions were used. Solution pH did not change before and after the reactions. Competition kinetic technique was used to determine the *k* value of $O_2^{\bullet-}$ and PCP^- using Adr as a reference compound. In a typical run, the mixture of PCP^- under a certain concentration and Adr at the fixed concentration of 200 μM was added into the working solution after a minute of UV irradiation. The working solution was continuously stirred by a magnetic stirrer (ZNCL−BS, Yuhua, China) at the speed of 400 rpm, and the temperature was kept at 20 ± 1 °C. The kinetic experiments were duplicated, and the data were obtained by averaging the replicates.

The rationale for the application of Adr as a reference compound is based on its unique reaction with $O_2^{\bullet-}$, producing adrenochrome (ADOM), and this product yields a characteristic absorbance feature at 485 nm:[4]

$$\text{Adr} + O_2^{\bullet-} \rightarrow \text{products} \quad (4)$$

The *k* for this reaction was reported to be 4.0×10^4 M^{-1} s^{-1} in a slightly alkaline solution at pH of 7.8.[5] Therefore, the *k* value between PCP^- and $O_2^{\bullet-}$ can be calculated based on the change of the absorbance (*A*) at 485 nm:[4]

$$\frac{A_0}{A} = 1 + \frac{k}{k_1}\frac{[PCP^-]}{[\text{Adr}]} \quad (5)$$

where A_0 and A are the change of absorbance in the absence and presence of Adr, respectively. It should be noted that no spectral interference from other substrates and reactions was observed.

DFT Calculations. In order to map possible reaction pathways for the degradation of PCP^- by $O_2^{\bullet-}$ under a non-steady state condition, DFT calculation was performed to

investigate this reaction on the molecular level. DFT provides a unique and powerful tool to study kinetics and mechanisms of the radical–induced bimolecular reactions.[6-8] First, Spartan'14 software package (version 1.1.4) with the Merck molecular force field (MMFF) was used for global minimum search of PCPs. Then, all subsequent calculations were carried out using the Gaussian 09 program package (Revision C.01). Possible pathways, including single electron transfer (SET) and bimolecular nucleophilic substitution (S_N2) were calculated. Transition state (TS) species are the key element to understand the reactivity and reaction of $O_2^{\bullet-}$ through the exploration of potential energy profiles.[9] Thus, the geometry structures of all the species including TSs were optimized at CAM–B3LYP/6–31+G** level of theory.[10] Vibrational frequencies were computed at the same level of theory. The selection of CAM–B3LYP was based on its feature for a better localization of the charges, avoiding calculation artifacts for $O_2^{\bullet-}$.[11] The solvation effect is considered using the Solvation Model based on Density (SMD) with water.[12] Then, high–level single–point energy calculations at the SMD/CAM-B3LYP/6-311++G** level of theory were performed based on the resulting geometries for the calculation of thermodynamic properties, including enthalpy change ΔH_R° (kcal mol^{-1}), Gibbs free energy change ΔG_R° (kcal mol^{-1}), and the activation energy $\Delta^\ddagger G^\circ$ (kcal mol^{-1}). Intrinsic reaction coordinate (IRC) method was used to ensure the resulting TSs connected both reactants and products.

We also mapped out the atomic charges of PCP^- with the Hirshfeld charge (q_A) distribution,[13] which is from the first-order information gain (I_G) upon the formation of a molecular system from its composing ingredients. The intrinsic information of a molecule such as regioselectivity, electrophilicity, and nucleophilicity, can be obtained from I_G, and is derived from:

$$I_G \approx \sum_A \int \left(\rho_A(r) - \rho_A^0(r)\right) dr = -\sum_A q_A \quad (6)$$

where $\rho_A(r)$ is the electron density on an atom/group A in that molecule, while $\rho_A^0(r)$ is the reference electron density of the same atom/group. In eqn. 6, q_A is the Hirshfeld charge on the atom/group A. With the first-order approximation, the information before and after upon a formation of that molecule is conserved. Thus, one arrives at eqn. 7 for q_A.

$$I_G \approx -\sum_A q_A \equiv 0 \quad (7)$$

In this study, Multiwfn 3.6 program was used to calculate the Hirshfeld charge of PCP^- using the resulting checkpoint file from the above Gaussian calculations as the input file.[14]

Further reactions of resulting products and $O_2^{\bullet-}$

The S_N2 reaction of $O_2^{\bullet-}$ with PCP results in the formation of a PCP-peroxyl radical. The peroxyl radical would be expected to further react with the solvent water, forming a PCP-peroxide (Fig. S2 (a)). The PCP-peroxide is susceptible to O-O homolytic bond cleavage to form a PCP-oxy radical. Then, the PCP-oxy radical reacts with water to form a PCP-hydroxide (reaction not shown) or with a hydroxyl radical (generated by previous reaction steps) to form a PCP-dioxy radical. Rearrangement of the electronic structure will form a tetrachloroquinone (TCQ). A similar process could be also possible for the ortho peroxyl radical product. The reaction modes for meta peroxyl radical are in a similar manner, initial formation of a peroxide, homolytic cleavage of the resulting O-O bond, and subsequent formation of the PCP-hydroxide (Fig. S2 (b)).

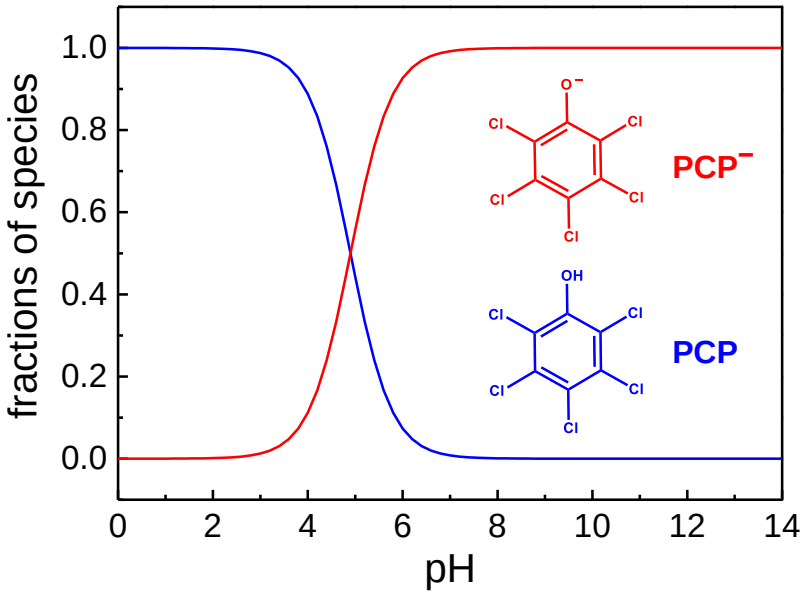

Fig. S1. The fraction of PCP and PCP^- as function of pH.

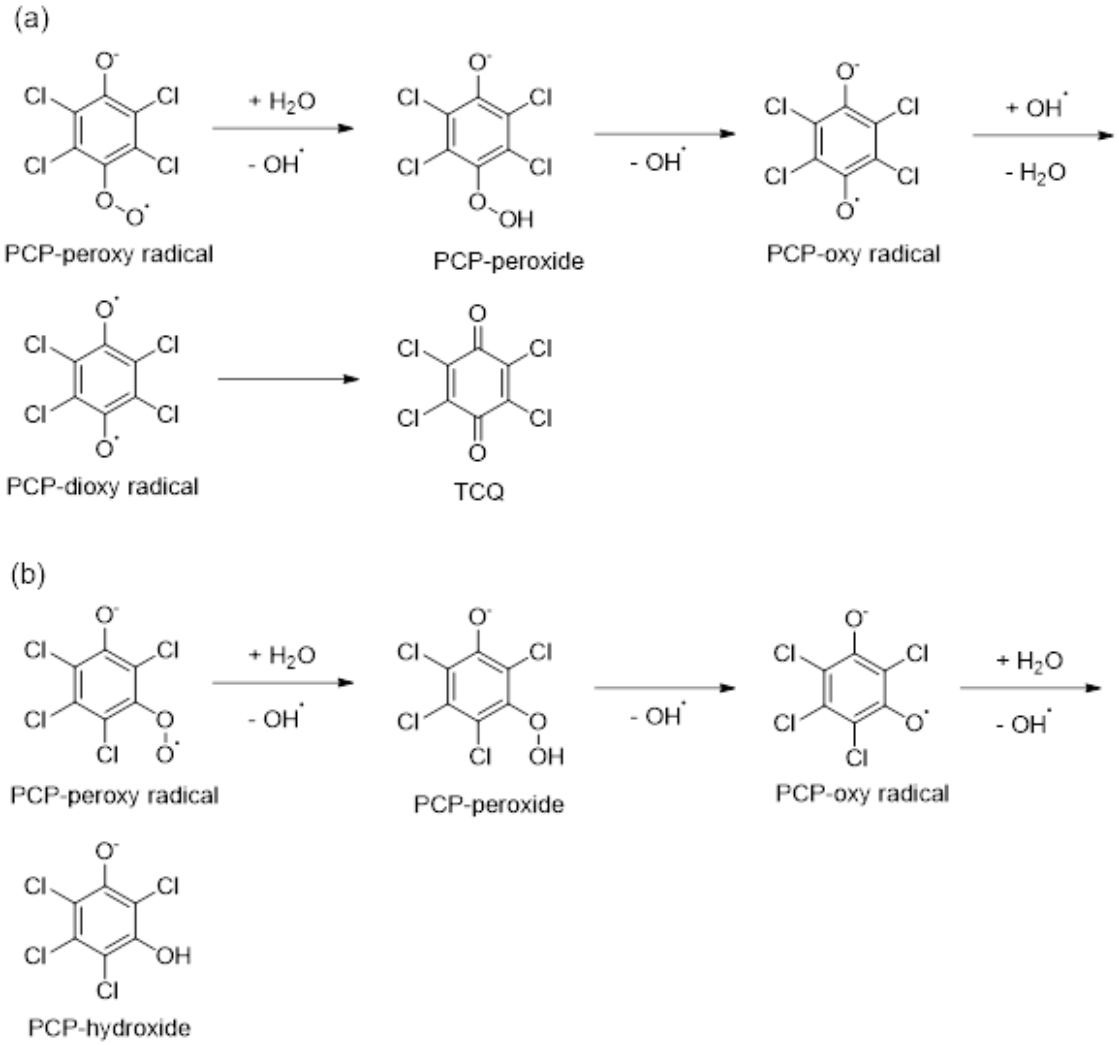

Fig. S2. Further possible reaction schemes for para-PCP-peroxyl radical (a), and meta-PCP-peroxyl radical (b).

Table S1. Cartesian coordinates (Å) for TS species at C3.

atom	X	Y	Z
O	-0.41927	-2.83192	0.10068
C	-0.13653	-1.60551	0.08847
C	-1.19476	-0.57282	0.10975
C	-0.85265	0.77407	0.09572
C	0.49571	1.21951	0.06701
C	1.50873	0.28762	0.05272
C	1.18504	-1.08867	0.05870
Cl	-2.14972	1.97065	0.09516
Cl	0.85732	2.94203	0.08573
Cl	3.19395	0.80503	0.04536
Cl	2.47804	-2.28857	0.01734
O	-2.27786	-0.95422	-1.32209
O	-1.75024	-0.47084	-2.39511
Cl	-2.64160	-1.07793	1.29158

Table S2. Cartesian coordinates (Å) for TS species at C4.

atom	X	Y	Z
O	0.68244	3.01271	-0.03039
C	0.47783	1.76871	-0.05185
C	-0.82634	1.17060	-0.09602
C	-1.09227	-0.20332	-0.12713
C	0.02183	-1.08232	-0.12065
C	1.31410	-0.56259	-0.07826
C	1.55438	0.80250	-0.05995
Cl	-2.18324	2.29154	-0.09245
Cl	-0.25900	-2.81610	-0.10838
Cl	2.67979	-1.68167	-0.06663
Cl	3.19075	1.44668	-0.04803
O	-2.17312	-0.68606	1.36105
O	-1.49584	-0.52171	2.44582
Cl	-2.53447	-0.75816	-1.27326

Table S3. Cartesian coordinates (Å) for TS species at C5.

atom	X	Y	Z
O	0.005054	3.242629	-0.069335
C	0.003158	1.971652	-0.067696
C	1.186888	1.163635	-0.065418
C	1.184992	-0.233472	-0.084971
C	-0.001139	-0.96957	-0.120777
C	-1.185105	-0.230006	-0.085226
C	-1.182918	1.167128	-0.065928
Cl	2.707626	2.044764	-0.042534
Cl	2.702711	-1.118861	-0.065874
Cl	-2.705426	-1.110934	-0.067033
Cl	-2.701062	2.05272	-0.043953
O	-0.007722	-1.631419	2.447769
O	-0.003429	-2.267214	1.329468
Cl	-0.003055	-2.5717	-1.352554

Table S4. The enthalpy change ΔH_R° (kcal mol^{-1}), Gibbs free energy change ΔG_R° (kcal mol^{-1}), and activation energy $\Delta^\ddagger G^\circ$ (kcal mol^{-1}) calculated at SMD/CAM–B3LYP/6–311++G**//CAM–B3LYP/6–31+G** level of theory for $O_2^{\bullet-}$ reacting with PCP^-.

pathway	reaction	comment	ΔG_R°	ΔH_R°	$\Delta^\ddagger G^\circ$
SET	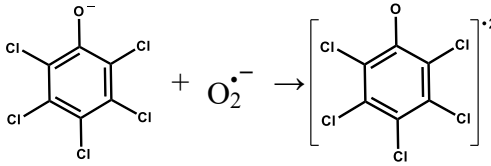	$O_2^{\bullet-}$ losing an electron	29.8	33.6	30.1
	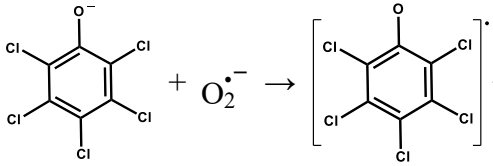	$O_2^{\bullet-}$ gaining an electron	52.3	52.4	220
S_N2	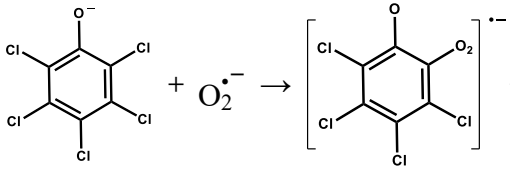	$O_2^{\bullet-}$ substituting Cl^- on ortho-position	-33.0	-24.4	19.0
	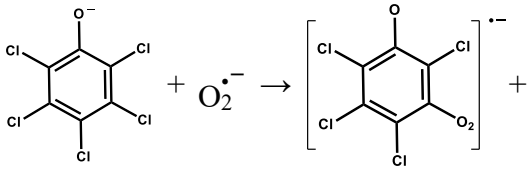	$O_2^{\bullet-}$ substituting Cl^- on meta-position	-31.3	-22.1	14.2
	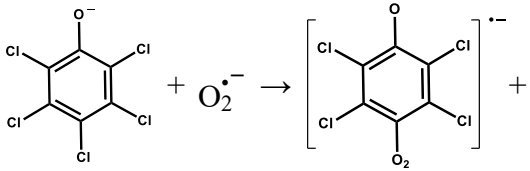	$O_2^{\bullet-}$ substituting Cl^- on para-position	-31.1	-23.9	21.3

References

1. T. M. Xie, K. Abrahamsson, E. Fogelqvist and B. Josefsson, *Environ. Sci. Technol.*, 1986, **20**, 457-463.
2. Z. Luo, M.-Y. Tseng, D. Minakata, L. Bai, W.-P. Hu, W. Song, Z. Wei, R. Spinney, D. D. Dionysiou and R. Xiao, *Chem. Eng. J.*, 2021, **410**, 128181.
3. B. H. Bielski and P. C. Chan, *J. Biol. Chem.*, 1976, **251**, 3841-3844.
4. W. Bors, C. Michel, M. Saran and E. Lengfelder, *Z. Naturforsch. C*, 1978, **33**, 891-896.
5. K. Asada and S. Kanematsu, *Agr. Biol. Chem.*, 1976, **40**, 1891-1892.
6. D. Minakata and J. Crittenden, *Environ. Sci. Technol.*, 2011, **45**, 3479-3486.
7. R. Xiao, M. Noerpel, H. Ling Luk, Z. Wei and R. Spinney, *Int. J. Quantum Chem.*, 2014, **114**, 74-83.
8. R. Xiao, L. He, Z. Luo, R. Spinney, Z. Wei, D. D. Dionysiou and F. Zhao, *Sci. Total Environ.*, 2020, **710**, 136333.
9. E. Wigner, *Trans. Faraday Soc.*, 1938, **34**, 29-41.
10. T. Yanai, D. P. Tew and N. C. Handy, *Chem. Phys. Lett.*, 2004, **393**, 51-57.
11. L. Lespade, *J. Theor. Chem.*, 2014, **2014**, 740205.
12. A. V. Marenich, C. J. Cramer and D. G. Truhlar, *J. Phys. Chem. B*, 2009, **113**, 6378-6396.
13. F. L. Hirshfeld, *Theor. Chim. Acta*, 1977, **44**, 129-138.
14. T. Lu and F. Chen, *J. Comput. Chem.*, 2012, **33**, 580-592.